Contents lists available at ScienceDirect

Arabian Journal of Chemistry

journal homepage: www.ksu.edu.sa

Original article

Potential of injectable psoralen polymeric lipid nanoparticles for cancer therapeutics

Fengjie Liu [a,1], Yuanyuan Huang [b,1], Xiujuan Lin [c,1], Qianwen Li [a], Idoia Gallego [d,e,f], Guoqiang Hua [g], Nadia Benkirane-Jessel [g], José Luis Pedraz [d,e,f,h], Panpan Wang [i,*], Murugan Ramalingam [d,e,f,h,j,*], Yu Cai [a,*]

[a] State Key Laboratory of Bioactive Molecules and Druggability Assessment, Jinan University / International Cooperative Laboratory of Traditional Chinese Medicine Modernization and Innovative Drug Development of Ministry of Education (MOE) of China / Guangdong Key Lab of Traditional Chinese Medicine Information Technology / School of Pharmacy, Jinan University, Guangzhou 510632, Guangdong, China
[b] VIP Department, State Key Laboratory of Oncology in South China, Guangdong Key Laboratory of Nasopharyngeal Carcinoma Diagnosis and Therapy, Guangdong Provincial Clinical Research Center for Cancer, Sun Yat-sen University Cancer Center, Guangzhou 510060, Guangdong, China
[c] The First Clinical Medical School of Guangzhou University of Chinese Medicine, Guangzhou 510405, Guangdong, China
[d] NanoBioCel Group, Department of Pharmacy and Food Sciences, Faculty of Pharmacy, University of the Basque Country (UPV/EHU), 01006 Vitoria-Gasteiz, Spain
[e] Bioaraba Health Research Institute, Jose Atxotegi, s/n, 01009 Vitoria-Gasteiz, Spain
[f] Biomedical Research Networking Centre in Bioengineering, Biomaterials and Nanomedicine (CIBER-BBN), Institute of Health Carlos III, 28029 Madrid, Spain
[g] French National Institute of Health and Medical Research (INSERM), UMR 1260, Regenerative Nanomedicine (RNM), 1 Rue Eugène Boeckel, 67000 Strasbourg, France
[h] Joint Research Laboratory (JRL) on Bioprinting and Advanced Pharma Development, A Joint Venture of TECNALIA (Basque Research and Technology Alliance), Lascaray Research Center, University of the Basque Country (UPV/EHU), 01006 Vitoria-Gasteiz, Spain
[i] The First Affiliated Hospital of Jinan University, Guangzhou 510632, Guangdong, China
[j] IKERBASQUE, Basque Foundation for Science, 48013 Bilbao, Spain

ARTICLE INFO

Keywords:
Polymer lipid nanoparticles
Psoralen
Pharmacokinetics
Plasma protein binding rate
Cancer

ABSTRACT

Triple-negative breast cancer (TNBC) is the most malignant subtype of breast cancer (BC) with a poor prognosis. Currently, chemotherapy and neoadjuvant chemotherapy continue to have limited efficacy in TNBC. With the deepening of research, nano targeted therapy shows a good application prospect in TNBC. Psoralen (PSO), an active component of Psoralea corylifolia, has significant advantages in inhibiting the growth of TNBC, but its poor solubility hampers its clinical practice. In this study, injectable psoralen polymer lipid nanoparticles (PSO-PLNs) were developed to deliver the hydrophobic drug to the target site and improve bioavailability. These nanoparticles were fully characterized in terms of morphology, particle size, surface zeta potential, encapsulation efficiency, drug loading, stability, and in vitro release profile. Besides, structural characteristics were determined by ultraviolet (UV) and infrared spectroscopy. Finally, in vivo pharmacokinetic studies of PSO-PLNs were performed in rats. The characteristic absorption of PSO and PSO-PLNs appeared in UV, indicating that PSO-PLNs had encapsulated PSO; there was no obvious characteristic absorption of PSO in infrared spectra, indicating that PSO was mostly encapsulated in the nano-shell. PSO-PLNs could maintain stable physicochemical properties for 1.5 months when stored at 4 °C. PSO-PLNs selectively released PSO at pH 6.5, and the sustained and controlled release effect was significantly different from that of PSO ($p < 0.01$). Pharmacokinetic studies in vivo demonstrated that PSO-PLNs could improve PSO bioavailability by increasing blood drug concentration and plasma protein binding rate. In summary, injectable PSO-PLNs could be considered as promising delivery system for advanced cancer therapeutics.

* Corresponding authors.
E-mail addresses: 47605961@qq.com (P. Wang), rmurug2000@gmail.com (M. Ramalingam), caiyu8@sohu.com (Y. Cai).
[1] **Equal contribution:** These authors contributed equally to this work.

https://doi.org/10.1016/j.arabjc.2024.105947
Received 2 June 2024; Accepted 1 August 2024
Available online 5 August 2024

1. Introduction

Cancer is the main malignant disease that jeopardizes human health. Research data show that the incidence of BC is on the top of the list of malignancy incidence in women (Siegel et al., 2022; Giaquinto et al., 2022). TNBC is a special type of breast cancer with negative expression of estrogen receptor, progesterone receptor and human epidermal growth factor receptor 2. In comparison with other subtypes of breast cancer, TNBC is more aggressive, has shorter disease-free survival, and has higher recurrence, metastasis rate and mortality. Currently, clinical systemic treatment combined with surgery can only rely on chemotherapy. However, the toxicity of chemotherapy drugs, patient tolerance and tumor cell resistance can lead to treatment failure of TNBC (Dewi et al., 2022). Therefore, the lack of specificity of traditional treatments has promoted the exploration of other effective alternative antitumor drugs, which is the focus of current research and attention.

Nanodrug delivery systems, such as nanoparticles, can encapsulate hydrophobic anti-tumor drugs and improve their stability (Saha et al., 2020; Zou et al., 2021). Besides, can also enhance the therapeutic efficacy and reduce the toxic side effects by increasing the selectivity of anti-tumor drugs in vivo (Shi et al., 2023). The small size, in the nanometer range, and special structure of nanoparticles make them have unique advantages in improving drug absorption, distribution, metabolism, excretion and toxicity (Wang et al., 2022; Meng et al., 2021). Polymer lipid nanoparticles (PLNs) are a new type of drug delivery system developed in recent years. PLNs include three different functional components: (i) a biodegradable hydrophobic polymer core that can carry poorly water-soluble bioactive drugs and release them at a sustained rate; (ii) a stealth material that forms a hydrophilic shell that enables the particles evade recognition by immune system components and increase the systemic circulation half-life of the particles; (iii) the lipid monolayer at the interface of the hydrophobic core and hydrophilic shell prevents the carried drugs from freely diffusing out of the NPs and reduces water penetration into the NPs, thus improving Drug encapsulation rate, slowing down drug release from NPs (Zhang et al., 2008; Liu et al., 2021). As the structural framework, the polymer core has the characteristics of mechanical stability, controllable morphology, biodegradation, narrow particle size distribution and large specific surface area. Phospholipid shell has good biocompatibility, easy to combine with a variety of molecules, high drug loading and encapsulation efficiency, which is beneficial to the inclusion and delivery of hydrophobic drugs. PLNs have high permeability and retention effect, which makes them easy to accumulate in TNBC microenvironment and achieve cell targeted drug delivery (Yang et al., 2020; Du et al., 2019). Different administration strategies, such as oral, injectables (intravenous (IV), intraperitoneal, and intramuscular), and pulmonary inhalation, are all viable options for the delivery of PLNs (Sudhakaran et al., 2020; Li et al., 2021). The development of injectable nanodrug delivery systems is currently receiving considerable attention since they can improve the payload, avoid first-pass metabolism, and significantly improve the pharmacokinetic parameters of active pharmaceutical ingredients (Han et al., 2022). However, most of the PLNs preparation methods reported in the literature can only obtain a small amount of samples, and the properties of the samples obtained after the amplification process are quite different from those obtained by the original process, which is one of the reasons that limit the widespread application of PLNs as formulation carriers.

The innovative development of nanotechnology has enabled its wide use in the field of anti-tumor therapies, providing a new way to improve the bioavailability of drugs and targeting cancerous cells. Herbal medicine components have good antitumor potential. However, the improvement of encapsulating or delivering hydrophobic drugs to the target site, solubility, stability, and bioavailability of their effective components is one of the research focuses. As a drug dosage that can contain the active ingredients of traditional Chinese medicine, the application of nanotechnology in the field of traditional Chinese medicine is still in its initial stage. Among them, Shenqi Fuzheng, Aidi, Shenmai, Coix seed fat emulsion and other injections, as well as ginsenoside Rg3 capsules, norcantharidin tablets and other oral preparations, have been used in clinical treatments (Zhang et al., 2019; Xiao et al., 2018; Shi et al., 2015; Song et al., 2020; Pu et al., 2021; Pan et al., 2020), but there are still few traditional Chinese medicine nano-preparations used in TNBC treatment.

Psoralen (PSO) is the main active component of Psoralea corylifolia, which has an inhibitory effect on various types of tumors. Studies have shown that PSO can inhibit the proliferation and promote apoptosis of TNBC MDA-MB-231 cells (Wang et al., 2018; Jin et al., 2020; Wang et al., 2019; Wang et al., 2016). However, PSO is a furanocoumarin compound with poor aqueous solubility and low bioavailability, which limits its efficacy. In this sense, the use of nanomaterials to wrap PSO could overcome these issues (Yuan et al., 2019; Huang et al., 2018; Du et al., 2019; Liu et al., 2021; Li et al., 2021). In addition, the nano carrier could allow PSO release in a controlled and sustained way, improving the stability of the active substance and enhancing its bioavailability. PLNs have the advantages of both liposome and polymer nanoparticles, and they have great development prospect as drug carriers (Li et al., 2017). Screening and designing composition formulations are the key technical difficulties in the field of nano research (Yuan et al., 2018). In addition, there is still a lack of evidence on how nanoformulations change the pharmacokinetic characteristics of PSO in vivo and the relationship between these changes and its improved efficacy.

Therefore, this study proposes a new PLNs preparation process, which can obtain about 5 times the amount of samples of the general method, and these samples have good properties. Using PSO as a template drug, PSO-PLNs were prepared using the constructed process, and their physicochemical properties, pharmacokinetic properties and anti-breast cancer activity were comprehensively evaluated.

2. Materials and methods

2.1. Materials

PSO (purity 98 %) was purchased from Chengdu Pufei De Biotech Co., Ltd. 1,2-Distearoyl-*sn*-glycero-3-phosphoethanolamine-Polyethylene Glycol-2000 (DSPE-PEG2000) was purchased from AVT (Shanghai) Pharmaceutical Tech CO. Ltd. Poly(lactic-co-glycolic acid (PLGA) (ratio of lactide and glycolide is 50:50, Mw10000) was purchased from Jinan Daigang Bioengineering Co., Ltd. Soybean lecithin (PC) (medicinal excipients for injection) was provided by Shanghai Taiwei Pharmaceutical Corp., Ltd. Tween-80 and mannitol were provided by Shanghai Aladdin Biochemical Technology Co., Ltd. Methanol was purchased from Guangdong Guanghua Company. Acetonitrile was obtained from Thermo Fisher Scientific. PBS was purchased from Biyuntian Biotechnology Co., Ltd. Clarithromycin and paclitaxel (PTX) were obtained from Shanghai Aladdin Biochemical Technology Co., Ltd. Mannitol, trehalose, lactose and glucose was purchased from Shanghai Macklin Biochemical Co., Ltd.

2.2. Preparation and optimization

2.2.1. PSO-PLNs preparation

PSO-PLNs were prepared according to an emulsification-evaporation method (Du et al., 2019). 180.0 mg PC and 22.5 mg DSPE-PEG2000 were dissolved in 200 mL 4 % ethanol water (v/v), with 0.19 % Tween-80 (T-80) as the water phase and stirred at 70 °C. 15 mg PSO and 55 mg PLGA were dissolved in 10 mL acetonitrile to form the organic phase. The organic phase was evenly added into the water phase and stirred at 70 °C, 300 r/min for 2 h, then 1000 rpm centrifugation step for 5 min was carried out. The sample preparation was carried out under non-sterile conditions. The sample dispersion was sterilized by filtration through a 0.22 μm filter membrane before use. The particle size of the nanoparticles was measured to allow them to pass through the

sterilization filter membrane.

2.2.2. Optimal preparation of PSO-PLNs freeze-dried powder

Some studies have shown that lyophilization can significantly improve the storage stability of PLNs. Commonly used lyoprotectant include lactose, glucose, mannitol, trehalose, etc (Li et al., 2023). PSO-PLNs were lyophilized to facilitate storage stability as powder. To examine the effect of the type of lyoprotectant on the properties of PSO-PLNs lyophilized powder, 10 % of different types of lyoprotectant were added to the prepared PSO-PLNs aqueous dispersion. In order to examine the effect of the proportion of lyoprotectant on the properties of PSO-PLNs freeze-dried powder, 0 %, 2 %, 4 %, 6 %, 8 % and 10 % (w/v) of the best lyoprotectant were added to the prepared PSO-PLNs aqueous dispersion. To obtain the powder, the solutions were freezed at −80 °C overnight and freeze-dried for 24 h in a freeze dryer (Alpha 2–4 LD plus, Beijing Oriental Science & Technology Development Ltd.). After the lyophilization process, PSO-PLNs powder was dissolved in pure water to perform further assays.

2.3. Encapsulation efficiency

The encapsulation efficiency (EE) of PSO in PSO-PLNs was determined by ultrafiltration method and high performance liquid chromatography (HPLC) (Huang et al., 2018). Take a portion of the newly prepared PSO-PLNs dispersion, sonicate it for 5 min to break the emulsification, and filter it through an organic membrane filter. The PSO concentration in the filtrate was detected by HPLC. The total PSO content was measured as M_t. Another equal volume of PSO-PLNs dispersion was introduced into an ultrafiltration EP tube (30 KDa) and centrifuged at 1200 rpm for 30 min. The PSO concentration in the filtrate was detected by HPLC. The free PSO content was measured as M_f. The mass of the freeze-dried powder obtained after freeze-drying of all newly prepared PSO-PLNs dispersions is M.

Chromatographic conditions:

Chromatographic column: C18 reversed-phase chromatographic column (Agilent ZORBAX SB-C18, 250 × 4.6 mm, 5 μm); mobile phase: acetonitrile: water (55:45); detection wavelength: 245 nm; column temperature: 30 °C; flow rate: 1.0 mL/min; injection volume: 10 μL.

The encapsulation efficiency was obtained by the following formula (1):

$$\mathrm{EE}\,(\%) = \frac{M_t - M_f}{M_t} \times 100\% \quad (1)$$

The drug loading (DL) was obtained by the following formula (2):

$$\mathrm{DL}\,(\%) = \frac{M_t - M_f}{M} \times 100\% \quad (2)$$

In formula (1) & (2), M_t refers to the total content of PSO used in preparation. M_f refers to the content of free (not encapsulated) PSO measured by HPLC. M refers to the mass of the freeze-dried powder of prepared PSO-PLNs dispersions.

2.4. Characterization of nanoparticles

Dynamic light scattering is a common method to analyze the size of NPs (Filippov et al., 2023). The particle size distribution, polydispersity coefficient (PDI) and zeta potential distribution of NPs in the aqueous dispersion of PSO-PLNs with appropriate concentration were detected by Laser Nanometer Particle Size Analyzer (Nano ZS 90, Malvern). The morphology, aggregates and size of PSO-PLNs were observed by transmission electron microscope (TEM) (TECNAI 10, Royal Philips, Netherlands) (Filippov et al., 2023). The carbon-coated copper grid was placed in a droplet of PSO-PLN dispersion, immersed for 5 min, blotted with filter paper, stained with 2 % (w/v) phosphotungstic acid for 1 min, and air-dried. Absorption wavelength of PSO-PLNs, methanol and PSO were detected by ultraviolet spectrophotometer (UH5300, Beijing Huaxu Century Technology Co., Ltd). The sample powders (PLN, PSO, PSO + PLN and PSO-PLN) were mixed with KBr at a mass ratio of 1:100 under a baking lamp, ground in an agate mortar, and pressed into tablets. The transmittance of the samples in the wavenumber range of 400–4000 cm^{-1} was detected by fourier transform infrared spectroscopy (FTIR) (T/IR-480, JASCO, China), with the number of scans set to 32 and the resolution set to 4. After obtaining the spectrum, the atmospheric background was subtracted and the baseline correction was performed (Du et al., 2019).

2.5. Stability study

The storage conditions of aqueous dispersions of PSO-PLNs refer to most commercially available liquid liposome drug products, i.e. 2–8 °C (Sainaga Jyothi et al., 2022). The aqueous dispersion of PSO-PLNs with appropriate concentration was sealed in vials and placed in a 4 °C refrigerator and room temperature (approximately 25 °C). 3 batches of samples per condition. Take appropriate amounts of sample solutions on days 0, 7, 30, 45 and 120 to detect particle size distribution, PDI, zeta potential distribution and EE.

2.6. In vitro drug release

In vitro drug release experiments were performed using dialysis method (Solomon et al., 2017). Obtain 20 mL of PSO-PLNs and PSO water dispersion with the same PSO concentration, place them in a dialysis bag with a molecular weight of 10000–14000 Da, and then immerse the dialysis bag in 100 mL of release medium (water). For comparison, the amount of PSO used was consistent with the amount of PSO contained in PSO-PLNs. The amount of PSO contained in PSO-PLNs can be determined by HPLC. The entire device was placed in a constant-temperature shaker (rotation speed 100 r/min, temperature 37 °C). Take an appropriate amount of release medium at different time points (0.5, 1, 2, 4, 8, 12, 24, 36 h), detect the concentration of PSO by HPLC, and calculate the cumulative release amount. To increase the solubility of PSO, the release medium contains 0.02 % surfactant (Tween 80). Due to changes in cell metabolism, the pH of the tumor microenvironment is around 6.2–6.8, while the pH of blood is around 7.4 (Ding et al., 2022). To evaluate the selectivity of drug release from NPs, the release behavior under different pH conditions (7.4 and 6.5) was examined.

2.7. Pharmacokinetic study

2.7.1. Administration method and plasma sample processing

Thirty specific pathogen free (SPF) grade male Sprague Dawley rats, submitted to adaptive feeding for one week, were randomly divided into PSO group and PSO-PLNs group (n = 15 in each group). After fasting (free drinking water) for 12 h, 0.765 mg/kg, calculated as PSO, was injected into the tail vein. Afterwards, 300–500 μL of blood was collected through the tail vein at 5, 15, 30 min and 1, 2, 4, 6, 8, 12, and 24 h after administration, respectively. The plasma was placed in a sodium heparin centrifuge tube and centrifuged at 4000 r/min for 15 min to obtain the supernatant. Clarithromycin was dissolved in methanol to prepare an internal standard solution with a mass concentration of 80 ng/mL. The PSO/PSO-PLN freeze-dried powder plasma sample was first thawed in a 4 °C refrigerator, and then the PSO/PSO-PLN freeze-dried powder plasma sample was vortexed for 1 min. Take 100 μL of PSO/PSO-PLN plasma sample and add 10 μL of Cl internal standard solution. Then, extract with ethyl acetate, 290 μL/time, 3 times. Combine the extracts, blow dry with liquid nitrogen, and reconstitute with 100 μL methanol. The reconstituted sample is the PSO/PSO-PLN plasma sample test solution.

2.7.2. Plasma drug concentration

Blood drug concentration at each time point was determined by

UPLC-MS/MS (Zhao et al., 2020). UPLC column temperature was set at 35 °C, and the mobile phase was water containing 0.1 % formic acid-acetonitrile. The flow rate was 0.4 mL/min and the injection volume was 5 μL. Gradient elution conditions were shown in Table 1. See Table 2 for mass spectrum conditions.

The average blood concentration–time curve was represented in a graph with time as the abscissa (X) and rat blood concentration as the ordinate (Y). PK Solver software was employed to calculate pharmacokinetic parameters in terms of peak time (T_{max}), maximum blood concentration (C_{max}), area under blood concentration–time curve (AUC), elimination half-life ($t\frac{1}{2}$) and mean residence time (MRT).

2.7.3. Determination of plasma protein binding rate

Commonly used methods for measuring plasma protein binding (PPB) include equilibrium dialysis, ultrafiltration, ultracentrifugation, etc (Barré et al., 1985). Considering the simplicity of operation, the ultrafiltration method was used in this study. Rat anticoagulated blood was obtained by collecting blood from the abdominal aorta, and the upper plasma was obtained by centrifugation (4 °C, 1500 r/min, 15 min). Dissolve the PSO standard and PSO-PLNs lyophilized powder in freshly prepared plasma respectively. For the detection of unbound free drugs (C_f), the solution was vortexed in a 37 °C water bath for 2 h, then placed in an ultrafiltration EP tube and centrifuged (4 °C, 8000 r/min, 15 min) to obtain plasma ultrafiltrate. Subsequently, 4 times the volume of acetonitrile was used to precipitate the protein in the plasma ultrafiltrate, and the supernatant was obtained by centrifugation (12000 r/min, 10 min). For the detection of total drugs (C_t), after the solution was vortexed in a 37 °C water bath for 2 h, the protein in the plasma ultrafiltrate was directly precipitated with 4 times the volume of acetonitrile, and the supernatant was obtained by centrifugation (12000 r/min, 10 min). Detect the concentration of PSO in the supernatant by HPLC, and the chromatographic conditions are the same as 2.3. PPB was calculated by the following formula (3).

$$\text{PPB}\,(\%) = \frac{C_t - C_f}{C_t} \times 100\% \quad (3)$$

In formula (3), *Ct* refers to the concentration of total PSO in blood. *Cf* refers to the concentration of free PSO in blood.

2.8. Animal husbandry

Thirty SPF grade male Sprague Dawley (SD) rats, 200 ± 20 g, were purchased from Guangdong Medical Laboratory Animal Center. 18–22 g BALB/c mice were purchased from the Guangdong Provincial Medical Experimental Animal Center and raised in the Medical Experimental Animal Center of Jinan University. Animal experiments were approved by the Experimental Animal Ethics Committee of Jinan University (IACUC-20210830-05). The SD rats were allowed to eat and drink freely under a temperature of 22 ± 2 °C, a humidity of 50 ± 10 %, an SPF environment, with a 12 h light/dark cycle.

2.9. Construction of tumor-bearing mouse models

Breast cancer 4T1 cell line (Procell Life Science & Technology Co., Ltd. CL-0007) from mouse BALB/c strain (Nanjing Keygen Biotech Co., Ltd) was cultured in RPMI-1640 medium (Thermo Fisher Scientific, Gibco) containing 10 % fetal bovine serum and 1 % penicillin–streptomycin in a humid incubator at 37 °C and 5 % CO_2. At passages P6-P10, 4T1 cells were dettached with 0.25 % trypsin-EDTA (Gibco, 25200056), collected, counted, and resuspended with matrix gel (ABW, 0827245) diluted 1:1 in PBS, to obtain a final cell density of 1×10^7cells/mL.

After alcohol disinfection, 200 μL cell suspension was injected subcutaneously into the right axillary side (n = 5 mice). After the tumor grew to about 1000 mm^3, the mice were sacrificed, the tumor blocks were removed and chopped, then transferred to a sterilized glass mortar, added with 5–8 mL phosphate buffer saline (PBS, pH 7.4), ground for 5 min, let stand, and the supernatant was centrifuged at 1000 rpm for 5 min to collect cells, and then resuspended with PBS. The remaining tissue blocks were ground 3–5 times, the collected cells were incorporated, centrifuged again, and finally resuspended with normal saline to a higher concentration. The obtained cell solution was injected into the subcutaneous right axilla of mice to be modeled.

Table 1
UPLC gradient elution conditions.

Time (min)	A (Water containing 0.1 % formic acid) (%)	B (Acetonitrile) (%)
0–2	95–88	5–12
2–4	88–85	12–15
4–8	85–65	15–35
8–9	65–60	35–40
9.01–13	0	100
13.01–16	95	5

Table 2
Mass spectrometry detection conditions.

Sample	Precursor ions (*m/z*)	Daughter ions (*m/z*)	CE (V)	DP (V)
PSO	187.7	132.1	31.33	80
Clarithromycin	747.8	158.4	30	80
Clarithromycin	747.8	558.4	30	80
Clarithromycin	747.8	590.3	24	80

2.10. Nanoparticles injection and anti-tumor efficacy analysis

Eighty mice were randomly divided into 8 groups: normal mice group, models group, PLNs group, free PSO group, low-dose PSO-PLNs group, medium-dose PSO-PLNs group, high-dose PSO-PLNs group, and PTX (positive control). PTX was administered intraperitoneally at a dose of 3 mg/kg, once every 2 days. PSO was administered intraperitoneally at a dose of 6 mg/kg, once a day. PSO-PLNs was administered by caudal vein at doses of 3 (L, low dose), 6 (M, medium dose) and 9 (H, high dose) mg/kg, once a day. The administration period was 15 days, the body weight of mice was recorded every 2 days, the long diameter 'a' and short diameter 'b' of the tumor were monitored, and the tumor volume was calculated by the formula: $V = 0.5 \times a \times b^2$. After the experiment, the tumors were dissected and weighed, and the average tumor inhibitory rate of each group was calculated by the formula (4):

$$\text{Tumor inhibitory rate}(\%) = \frac{W_m - W_n}{W_m} \times 100\% \quad (4)$$

In the formula (4), W_m is average tumor weight of model group, W_n is average tumor weight of test group.

2.11. Statistical analysis

All experimental tests were performed in three replications. All the experimental data were expressed as mean ± standard deviation (SD). Statistical analysis was done using GraphPad Prism 6.0 software and * $p < 0.05$, ** $p < 0.01$, *** $p < 0.001$ and **** $P < 0.0001$ were considered to indicate a statistically significant difference.

3. Results

3.1. Investigation on the lyophilized protective agent

The results in Fig. 1A showed that the product obtained without adding lyoprotectant was not powdery and stuck to the bottom. The product obtained by adding 10 % mannitol was in the form of fluffy powder. The results in Fig. 1B showed that the powder obtained after adding trehalose, lactose, and glucose still appeared to be sticky. In

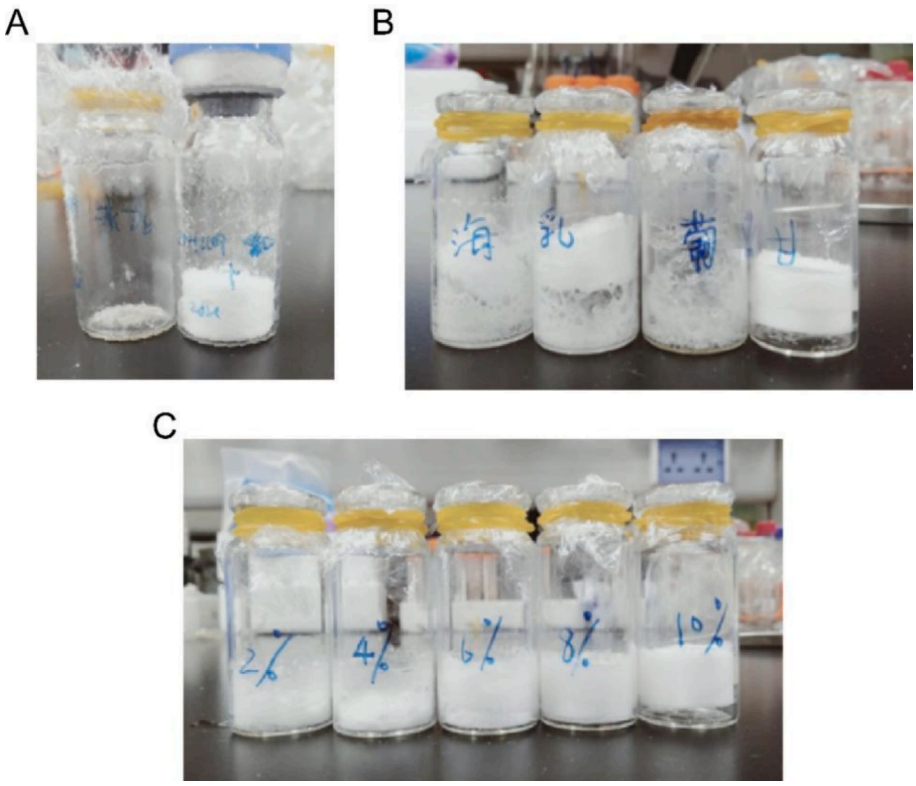

Fig. 1. Examination of lyophilization protectant types and dosages. A: PSO-PLNs lyophilized powder obtained by direct lyophilization of PSO-PLNs on the left and PSO-PLNs lyophilized powder obtained by adding 10 % mannitol on the right; B: PSO-PLNs lyophilized powder lyophilized by adding 10 % trehalose, lactose, glucose and mannitol, respectively; C: PSO-PLNs lyophilized powder obtained by adding 2 %, 4 %, 6 %, 8 % and 10 % mannitol in order from left to right.

contrast, the addition of mannitol resulted in a powder that was fluffy and dry with little stickiness to the walls. Therefore, mannitol was an ideal freeze-drying protectant among the tested species. The results in Fig. 1C showed that as the concentration of added mannitol increased, the wall sticking of the obtained powder decreased. The results in Table 3 showed that the particle size, EE and DL detected after reconstitution of the freeze-dried powder obtained by adding 8 % mannitol were ideal. A study investigated the effect of the combination of sucrose or trehalose with mannitol on the properties of nanoparticles, and the results showed that the best stability was achieved at a total concentration of 10 %. In terms of action, mannitol provided an elegant cake structure, sucrose was superior to trehalose in maintaining particle size during freeze-drying, and trehalose was more effective in keeping the particle size within limits during storage (Mitrović et al., 2023). This confirms our findings that among all the types of lyoprotectants investigated, mannitol had a good shaping effect and its optimal concentration was around 10 % (8 %).

Table 3
Particle size, polydispersity index (PDI), zeta potential, encapsulation efficiency and drug loading of freeze-dried PSO-PLNs using different concentrations of mannitol as lyoprotectant.

Mannitol concentration (%)	Particle size (nm)	PDI	Zeta potential (mV)	EE (%)	DL (%)
2	162.6 ± 2.4	0.224 ± 0.007	−(23.13 ± 1.12)	72.5	0.551
4	153.0 ± 0.6	0.234 ± 0.021	−(0.009 ± 0.17)	24.8	0.305
6	148.2 ± 0.4	0.182 ± 0.006	−(11.45 ± 2.43)	22.2	0.227
8	140.1 ± 1.8	0.217 ± 0.025	−(15.03 ± 2.27)	68.5	0.175
10	132.7 ± 0.7	0.234 ± 0.008	−(20.70 ± 1.67)	21.4	0.170

3.2. Characterization

As can be seen from Fig. 2A, PSO-PLNs present a transparent colloid solution with light blue opalescent light. The morphological analysis under TEM showed that PSO-PLNs were spheroid-like with no aggregates(Fig. 2B).The average encapsulation efficiency of PSO-PLNs was 74.38 %±1.66 % (RSD < 2 %).The average particle size of PSO-PLNs was 134.4 ± 10.12 nm (Fig. 2C) and PDI was 0.158 ± 0.012 (PDI $<$ 0.3), indicating that PSO-PLNs have uniform particle size and dispersion. Zeta potential of PSO-PLNs was −16.3 ± 2.8 mV (Fig. 2D). Fig. 2E shows that both PSO and PSO-PLNs had a strong absorption peak at 245 nm, which is the characteristic absorption of PSO, indicating that PSO-PLNs contained PSO. Methanol was only weakly absorbed at 230 nm, indicating that methanol as solvent would not affect the detection of PSO. FITR spectra showed that the characteristic absorption peak of α-furanone of 1716 cm^{-1} and the absorption of conjugated double bond of 1632 cm^{-1} aromatic ring appeared after physical mixing of PSO and PLNs carrier (Fig. 2F). The characteristic peak of 2363 cm^{-1} appeared in the spectra of PSO, PLN and PSO-PLNs, but the characteristic absorption of 3156 cm^{-1} only appeared in PSO and PLNs, indicating that most PSO was wrapped in PSO-PLNs.

3.3. Stability

Aqueous dispersions of PSO-PLNs stored in sealed vials were placed at 4 °C and 25 °C. The particle size, potential and drug encapsulation efficiency of the samples were detected on days 0, 7, 30, 45 and 120. The results in Fig. 3 show that under 4 °C conditions, all detected physical and chemical properties of PSO-PLNs remained stable on days 7, 30, and 45, with no significant difference from the initial detection state. Under the condition of 25 °C, the detected physical and chemical properties

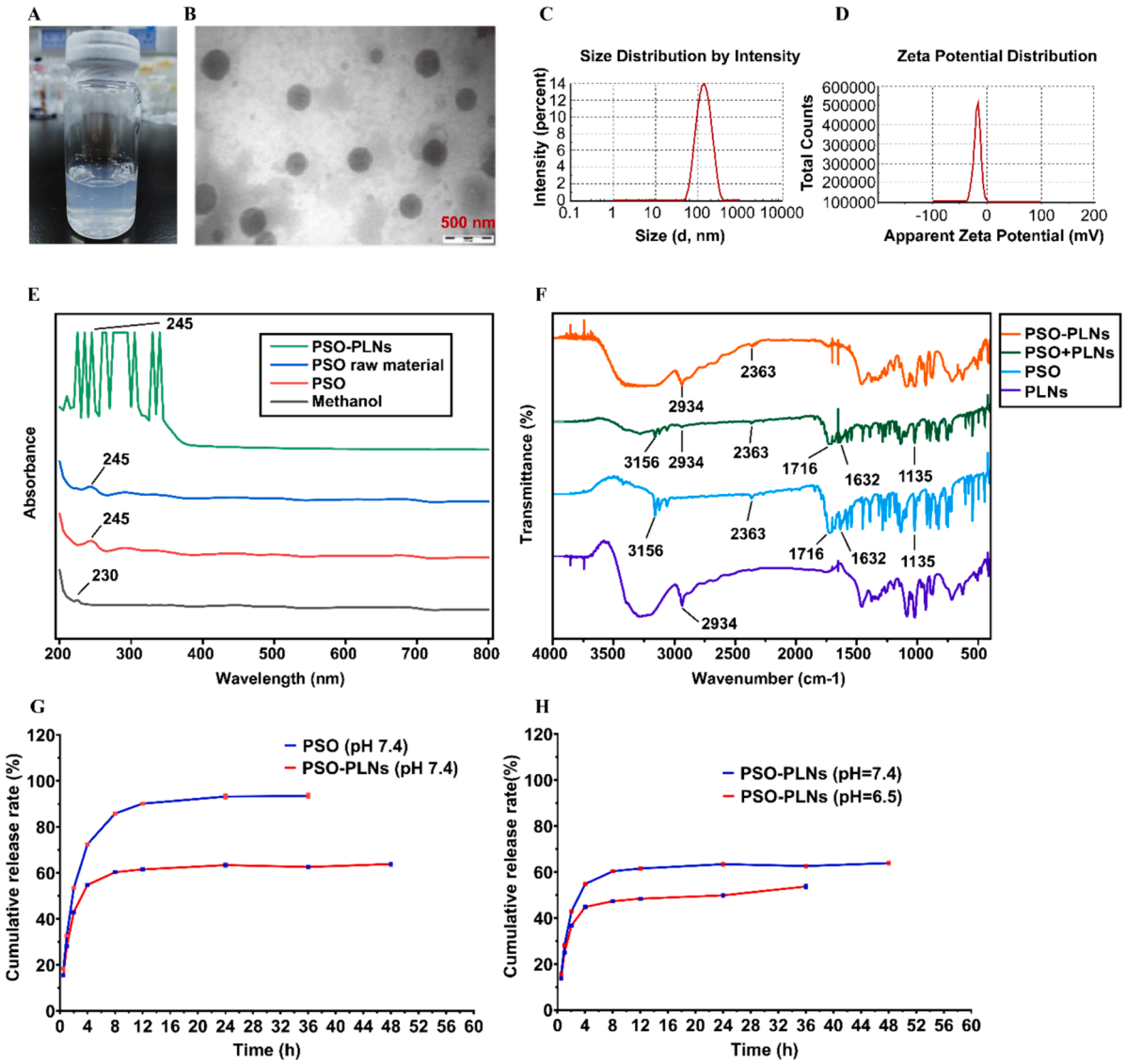

Fig. 2. PSO-PLNs physical and chemical properties. A:Visual aspect of PSO-PLNs solution; B: TEM image of PSO-PLNs; Scale bar: 200 nm;C: Particle size of PSO-PLNs; D: Zeta potential of PSO-PLNs; E: UV absorption spectra of PSO-PLNs; F: FTIR spectra of PSO-PLNs, PSO + B-PLNs, PSO and PSO-PLNs; G: In vitro release of PSO and PSO-PLNs at pH = 7.4; H: In vitro release of 5-fold PSO-PLNs at pH = 7.4 and 6.5.

remain stable within 7 days.

3.4. *In vitro release*

To study the sustained release effect of PSO-PLNs at different pH conditions, the in vitro release rate of PSO from PSO-PLNs was monitored in PBS (pH7.4, 6.5) within 36 h. As can be seen from Fig. 2G-H, under pH 7.4, the cumulative release rate of PSO exceeded 60 % within 4 h, and the release rate was almost complete within 24 h. The cumulative release of PSO-PLNs at 36 h was only over 60 %. The cumulative release of PSO in PSO-PLNs was the highest at pH 6.5, indicating that PSO-PLNs could release PSO rapidly in tumor microenvironment conditions, which proved that PSO-PLNs could selectively release drugs. 1, 2-distearoyl-*sn*-glycerol-3-phosphoethanolamine-polyethylene glycol (DSPE-PEG) is a lipid-polyethylene glycol copolymer composed of two different components: a hydrophilic block (PEG) and a hydrophobic phospholipid block consisting of two long fatty acyl chains (phosphatidylethanolamine, DSPE). PEG and DSPE are connected through urethane bonds, which can be hydrolyzed under acidic conditions and thus exhibit pH sensitivity (Zhang et al., 2008). In our study, DSPE-PEG was used to insert into the outer lipid layer to form a PEG stealth coating on the surface. Since the ester bond of DSPE-PEG is easily hydrolyzed in acidic media, it may lead to instability and destruction of the lipid bilayer and exposure of the PLGA core, showing pH-responsive release of the encapsulated drug. This may explain why PSO-PLNs released faster in pH 6.5 medium. When the pH was as low as 5.5, the release of PSO-PLN was slower than that of blood and normal tissues. This phenomenon has not been well explained. It may be related to the premature exposure of the hydrophobic PLGA core caused by the rapid degradation of PEG and lipid layers. Due to hydrophobic interactions, PSO may prefer to stay in the PLGA core rather than be released into water (Sánchez-Iglesias et al., 2012). Before a reliable conclusion can be drawn, in-depth analysis of particle changes is needed.

3.5. *Pharmacokinetic study*

3.5.1. *Blood concentration*

After single injection of PSO or PSO-PLNs through caudal vein in rats, the blood concentration at each time point was determined by UHPLC-MS. As shown in Fig. 4 and Table 4, the peak time (T_{max}) of PSO-PLNs

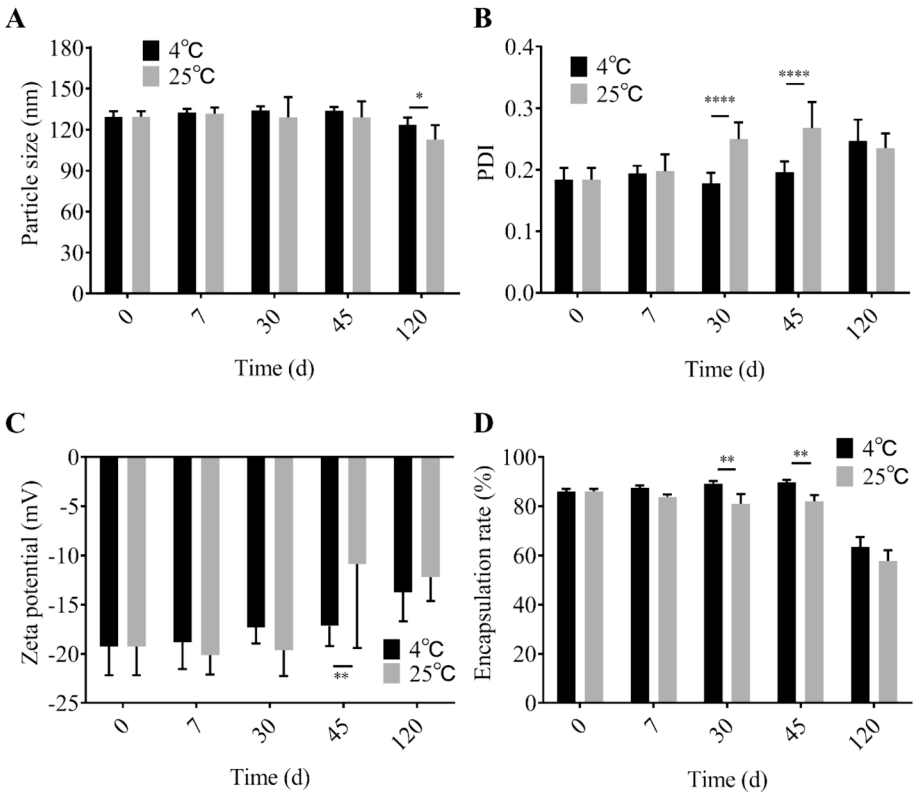

Fig. 3. Stability of 5-fold PSO-PLNs at different storage temperatures (n = 3). A: Particle size change of 5-fold PSO-PLNs at 4 °C and 25 °C; B: PDI change of 5-fold PSO-PLNs at 4 °C and 25 °C; C: Zeta potential change of 5-fold PSO-PLNs at 4 °C and 25 °C; D: Encapsulation efficiency change of 5-fold PSO-PLNs at 4 °C and 25 °C. (* $P < 0.05$ 4 °C vs. 25 °C; ** $P < 0.01$ 4 °C vs. 25 °C; **** $P < 0.0001$ 4 °C vs. 25 °C).

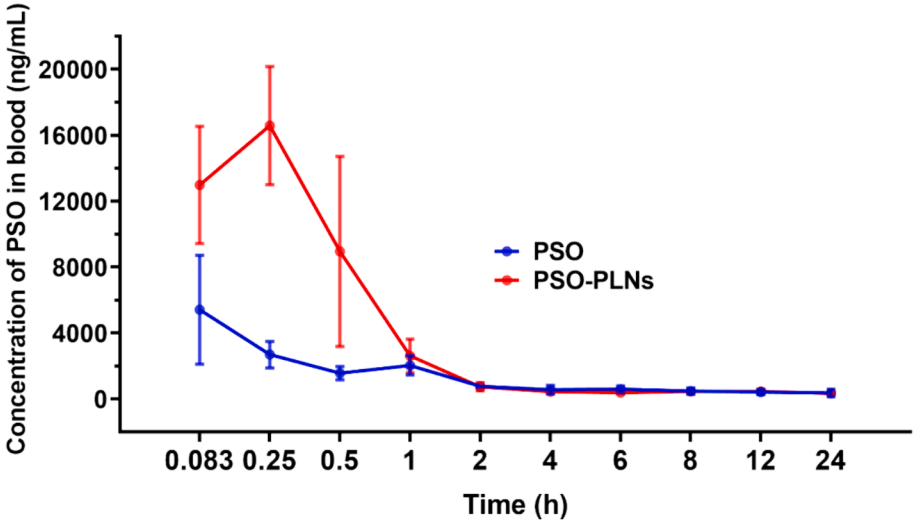

Fig. 4. Blood concentration–time curve after tail vein injection of PSO or PSO-PLNs in rats ($\bar{x} \pm s$, n = 4).

Table 4
Pharmacokinetic parameters after tail vein injection of PSO or PSO-PLNs in rats (($x^{-} \pm s$, n = 4)).

	T_{max}/h	C_{max}/ng/mL	AUC0-24 h/ng/mL·h	AUC0-∞/ng/mL·h	$t\frac{1}{2}$/h	MRT0-∞
PSO	0.35 ± 0.44	8694.34 ± 7241.27	15509.65 ± 4329.96	26142.48 ± 7752.31	23.85 ± 16.52	29.43 ± 21.23
PSO-PLNs	0.21 ± 0.08	13353.94 ± 6216.02	19683.94 ± 5555.12	28195.03 ± 7349.63	18.09 ± 13.88	21.62 ± 13.26

Note: Due to the differences in body weight, blood flow, metabolic activity, etc. among the animals and difficulty in consistent human operations, the standard deviation of the data was large. The results of this study need to be further verified.

was shorter than that of PSO, the peak concentration (C_{max}) was 1.54 times higher than that of PSO, and the area under the curve (AUC 0–24 h) was also increased to 1.27 times compared with that of PSO. The $t_{\frac{1}{2}}$ and mean residence time (MRT) indicated that PSO-PLNs could accelerate the absorption of PSO in vivo and improve the bioavailability.

3.5.2. Plasma protein binding rate

The binding rate of plasma protein is an important parameter in pharmacokinetic study, which can directly show the distribution, transport, elimination, and action intensity of drugs in vivo. It is generally believed that drugs cannot be transported across the membrane after binding to plasma proteins to form a complex. Only unbound drugs can diffuse passively outside the blood vessels or to the tissue sites where the drugs produce pharmacological effects. Therefore, it can be considered that free drugs are the "active drug" form in the blood and even the target. In addition, the adsorption of plasma proteins on the surface of nanoparticles may cause changes in the physical properties of the preparation, such as aggregation and charge neutralization, which may lead to biochemical activation of the systemic defense cascade and trigger elimination by the mononuclear phagocytic system. Therefore, for nanoformulations, having a lower plasma protein binding rate is often beneficial to its systemic circulation stability and therapeutic effect (Aggarwal et al., 2009). It was observed that plasma protein binding rate of PSO-PLNs was significantly higher than that of PSO ($p < 0.05$), indicating that PSO-PLNs can be fully transported in the blood, with slow elimination in vivo, sustained release for a long time, stable drug concentration, and hence, suggesting a better therapeutic effect (Table 5). By contrast, the low binding rate of PSO plasma protein indicated rapid elimination in vivo, short action time, unstable concentration, low stability and low pharmacodynamic effect. This may be one of the main reasons why the antitumor effect of PSO-PLNs could be superior to that of PSO.

3.5.3. PSO-PLNs inhibit breast cancer growth in 4T1 tumor-bearing mice

The antitumor efficacy of different formulations was evaluated by measuring the changes in the tumor volume and final tumor weight during the experiment. Body weight curve of mice is shown in Fig. 5A. The tumor growth curve of each group is shown in Fig. 5B. The inhibitory effect of PSO-PLNs on the growth of 4T1 breast cancer was evaluated using xenograft mouse model. As shown in Fig. 5C-D, the inhibitory rates of PLNs group, free PSO group, low-dose PSO-PLNs group, medium-dose PSO-PLNs group, high-dose PSO-PLNs group and PTX group were 10.83 %, 50.61 %, 64.98 %, 73.98 %, 83.66 % and 75.91 %, respectively. Compared with control group, tumor growth was significantly inhibited in all groups ($p < 0.05$) except PLNs group. Compared with PSO group, low-dose PSO-PLNs group, medium-dose PSO-PLNs group, high-dose PSO-PLNs group and PTX group had significant differences ($p < 0.05$). Compared with low-dose PSO-PLNs group, high-dose PSO-PLNs group had significant differences ($p < 0.001$). Compared with high-dose PSO-PLNs group, PTX group had no significant differences ($p > 0.05$). The results showed that PSO and PSO-PLNs inhibited the growth of breast cancer in 4T1 tumor-bearing mice, using PLNs to deliver PSO could improve the efficacy of PSO. Because PSO-PLNs increases the accumulation of PSO in tumor sites.

The effects of PSO as an anti-breast cancer agent in intro have been reported to include inhibition of growth, survival, drug resistance, and induction of cell cycle arrest and apoptosis (Panno and Giordano, 2014). Our study further confirmed that PSO can inhibit breast tumor growth in vivo. However, the anti-breast cancer growth effect of PSO-PLNs was not dose-dependent, which may be because the accumulation and release of drugs at the target site are affected by multiple factors, rather than simply increasing with the increase of applied concentration. Therefore, in-depth study of the in vivo fate of PSO-PLNs will be beneficial for understanding and improving its therapeutic effect (Shi et al., 2017). Although PSO-PLNs had considerable efficacy, they did not show outstanding advantages over traditional chemotherapeutic drug PTX. Previous studies have confirmed that PSO had the effect of reversing tumor chemotherapy resistance, which suggests the potential application of PSO-PLNs in combination with chemotherapeutic drugs (Liu et al., 2021).

Table 5
PSO and PSO-PLNs plasma protein binding rates ($n = 3$; $^*p < 0.05$).

	Ct (μg/mL)	Cf (μg/mL)	PPB (%)
PSO	2.90 ± 0.17	1.02 ± 0.01	64.70 ± 0.71
PSO-PLNs	2.80 ± 0.18	1.36 ± 0.28	50.61 ± 7.13*

4. Discussion

At present, breast cancer is still showing a trend of high incidence and high mortality worldwide. Due to the limitation of drug efficacy, innovative anti-TNBC drugs need to be developed urgently. In recent years, nanometer drug delivery systems preparation has become an ideal dosage form for the delivery of antitumor drugs due to its characteristics of improving bioavailability, reducing toxicity, targeting and slow and controlled drug release (Li et al., 2017). Systemic administration is one of the fastest ways of absorption. However, insoluble drugs are difficult to reach effective therapeutic concentration in vivo due to the limitation of solubility and injection volume. Injectable nanodrug delivery systems have the significant advantage of bypassing the gastrointestinal tract and reaching the bloodstream directly, enabling rapid and efficient drug absorption, avoiding first-pass metabolism and improving bioavailability (Ye et al., 2022). According to the characteristics of TNBC disease, the combination of traditional Chinese medicine with the characteristics of enhancing efficacy and decreasing toxicity is helpful to improve drug solubility, active targeting and increase efficacy, providing a new way for TNBC targeted therapy.

The active ingredient of traditional Chinese medicine PSO has a clear effect on anti-TNBC. Studies have shown that PSO can promote cell apoptosis, inhibit cell migration and invasion through IRAK1/NF-κB/FAK signaling pathway, and has a significant effect on the growth of TNBC and lung metastasis (Liu et al., 2021). PSO can also enhance the cytotoxic effects of doxorubicin (DOX) and reverse breast cancer resistance (Huang et al., 2018). In addition, PSO also plays an important role in cell metabolism by influencing the abundance of metabolites in mouse serum and urine to achieve tumor inhibition (Li et al., 2021). In order to improve the poor water solubility of PSO, based on the principle of infiltration and retention effect, PLNs were screened and PSO-loaded PLNs were innovatively constructed (Yuan et al., 2019; Huang et al., 2018; Du et al., 2019; Liu et al., 2021; Li et al., 2021; Li et al., 2017). PLN is a shell structure composed of phospholipid shell and polymer core, which has a promising application prospect due to its advantages of slow release, targeting, improved bioavailability and safety.

This study focused on a type of injectable PLNs loaded with PSO. In previous studies, we have proposed the preparation process of PSO-PLNs (Du et al., 2019). The difference from previous studies was that this study amplified the process to 5 times the original one and improved it. The reasons for this are, on the one hand, to increase the preparation volume; on the other hand, to explore the possibility of large-scale production. First, dynamic light scattering, IR, UV and other methods were used to characterize the physical and chemical properties of PSO-PLNs, confirming that they had the envisioned structural composition and appropriate size. Compared with our previous research results, the process used did not affect the particle size, surface potential and EE. However, when the process was scaled up 5x, some parameters must be changed to maintain product properties. In addition, the current process dosage is still far from reaching the minimum dosage for industrial production. This shows that the current preparation of PLNs still meets difficulties that need to be overcome before achieving large-scale production (Hu et al., 2016).

Subsequently, to improve storage stability, different lyoprotectants

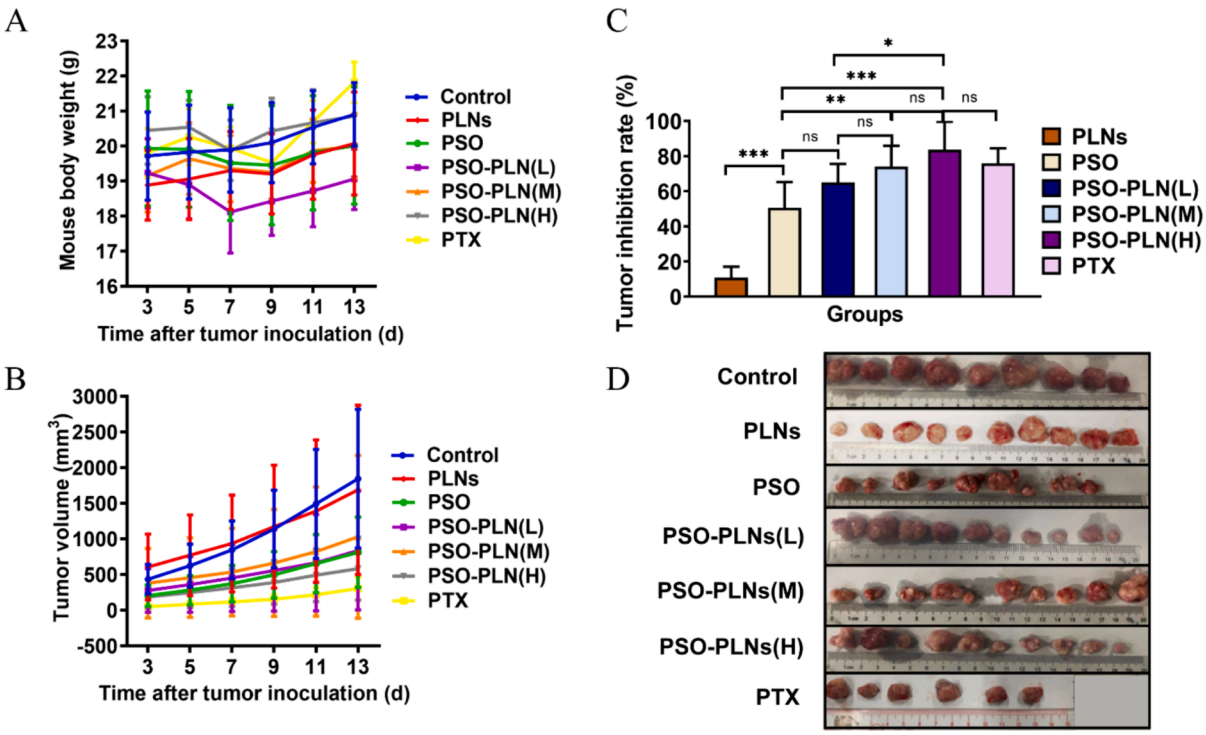

Fig. 5. PSO-PLNs inhibited the growth of breast cancer in 4T1 tumor-bearing mice. A. Body weight curve of mice; B. Tumor inhibition rate; C. Tumor growth curve of mice; D. Images of the tumor taken from the mice at day 13. Values are expressed as mean ± standard deviation(n = 10). p-values were calculated with One way ANOVA. *P < 0.05, **p < 0.01, ***P < 0.001, ****P < 0.0001. PLNs: Polymeric lipid nanoparticle; PSO: Psoralen; PSO-PLNs (L): Psoralen-loaded polymeric lipid nanoparticle (Low-dose); PSO-PLNs (M): Psoralen-loaded polymeric lipid nanoparticle (Medium-dose); PSO-PLNs (H): Psoralen-loaded polymeric lipid nanoparticle (High-dose); PTX: Paclitaxel. Note: Due to individual differences in animals and difficulty in consistent human operations, the standard deviation of the data was large. The results of this study need to be further verified.

were screened, and it was finally found that 8 % mannitol had a better morphology and maintained the physical and chemical properties of the NPs themselves. Some studies had also found that mixed freeze-drying protective agents can achieve multiple effects such as shaping and stabilization at the same time (Li et al., 2023). This suggests that research on freeze-drying protective agents can expand ideas. The prepared PSO-PLNs were investigated for up to 4 months of stability under two conditions, and it was found that they could be sealed and stored at 4 °C for 45 days without obvious property changes, and the properties began to change under the accelerated condition of 25 °C after 1 week of storage. Although our study did not strictly follow the standards for stability evaluation, that is, long-term stability experiments for more than 1 year and accelerated experiments for 6 months, it can provide a reference for further optimization of formulations and systematic stability evaluation in the future. In addition, the stability of the freeze-dried powder also needs to be investigated.

The tumor microenvironment has a lower pH (approximately 6.2 ~ 6.8) than normal tissue and blood, which provides ideas for the construction of many intelligent and responsive nanodrug delivery systems (Ding et al., 2022). Nanocarriers with pH-responsive degradation function have been shown to increase drug accumulation at tumor sites (Gou et al., 2023). This study examined the drug release kinetic characteristics of PSO-PLNs under pH 7.4 and 6.5 conditions. The results showed that PSO-PLNs released faster at pH 6.5, which may help them release more drugs at the tumor site. The DSPE-PEG2000 used was once again proven to be a material that imparts pH-responsive functionality to liposomes (Zhang et al., 2008).

To determine whether the carrier system based on PLNs improves the bioavailability of PSO, UPLC/MS was used to measure the drug concentration–time change curve in rat plasma after tail vein administration of PSO and PSO-PLNs. The results showed that compared with the injection of free PSO, the C_{max} and AUC of PSO in the blood were increased and T_{max} was shortened after the injection of PSO-PLNs. In fact, the purpose of the PLNs carrier system is to encapsulate PSO so that it can stably exist in the blood for a long time and pass through vascular endothelial cells at the tumor site. For the PSO-PLNs group, detecting large amounts of free PSO in the blood was undesirable, meaning premature leakage of the drug could occur. Therefore, the results of pharmacokinetic studies of PSO-PLNs may not provide useful conclusions. Studies on tissue distribution and cellular uptake in vivo may be more meaningful (Hoshyar et al., 2016). Nonetheless, our study confirmed that the PLNs-based carrier system could improve the bioavailability of PSO.

When administered systemically, nanoparticles encounter serum proteins in biological systems, resulting in the formation of a “protein corona” on the surface, which has been implicated in recent years as one of the confounding factors leading to limited clinical translation (Chen et al., 2020). It is generally accepted that once nanoparticles meet biological media, such as serum or plasma, their surfaces are modified by macromolecules, thereby converting their “synthetic properties” into so-called biological properties characterized by the specific proteins to which they are bound (Barbero et al., 2017). Our study showed that PSO-PLNs had lower PPB compared to free PSO. For anti-tumor nanodrug delivery systems, it is difficult to evaluate whether high or low PPB is beneficial or detrimental, depending on the designed function of the NPs and the drug’s mechanism of action. Therefore, further research into the types of proteins that bind to drugs is needed.

Finally, the anti-breast cancer activity of PSO-PLNs was evaluated through in vivo experiments. Consistent with our previous research results (Liu et al., 2021), the prepared PSO-PLNs had significant anti-breast cancer activity. This result mutually confirmed the results of the PPB study, indicating that PPB may affect the efficacy of PSO. PSO-PLNs may avoid being cleared by the mononuclear-phagocytic system by reducing the binding of certain plasma proteins and increasing their

accumulation in tumor sites. The lower tumor inhibition rate of PTX may be related to its poor bioavailability.

5. Conclusions

The optimized PSO-PLNs was a light blue opalescent colloid solution with an average particle size of 134.4 ± 10.12 nm, PDI of 0.158 ± 0.012 (PDI < 0.3) with uniform dispersion, zeta potential of −16.3 ± 2.8 mV, and the encapsulation efficiency of 74.38 ± 1.24 %. The type and dosage of PSO-PLNs lyoprotectant agent were investigated. The preparation of PSO-PLNs lyophilized protective agent should be made of 8 % mannitol and stored at 4 °C away from light. Compared with PSO raw material, PSO-PLNs were more stable under high temperature, high humidity, and strong light. In vitro release studies from PSO-PLNs showed that PSO could be selectively and rapidly released at pH 6.5 in the tumor microenvironment and slowly released at pH 7.4. The Tmax, Cmax and AUC 0–24 h of PSO-PLNs were higher than that of PSO, the $t_{\frac{1}{2}}$ and MRT was lower, the plasma protein binding rate was significantly higher than that of PSO ($p < 0.05$), and the bioavailability increased. In vivo experiments showed that PSO and PSO-PLNs could effectively inhibit the growth of 4T1 breast cancer mouse model. At high doses, the delivery of PSO by PLNs could improve the efficacy of PSO. The results showed that the preparation process used can obtain a relatively large amount of PLNs while maintaining the required physicochemical properties. The constructed PLNs can provide a promising nano-delivery system for poorly soluble small molecule drugs such as PSO to improve bioavailability. PSO-PLNs can provide a potential effective nano-drug for breast cancer treatment. Further functional improvement, safety, efficacy in different experimental models and mechanism of action of PSO-PLNs are the focus of future in-depth research.

6. Data Availability Statement

The original contributions presented in the study are included in the article, further inquiries can be directed to the corresponding authors.

7. Disclaimer

The statements, opinions and data contained in all publications are solely those of the individual author(s) and contributor(s) and not of MDPI and/or the editor(s). MDPI and/or the editor(s) disclaim responsibility for any injury to people or property resulting from any ideas, methods, instructions or products referred to in the content.

Supplementary Materials

All data generated or analyzed during this study are included in this published article.

Funding

This work was supported by the International Programs & Strategic Innovative Programs of National Key Research and Development Program of China [Grant number 2023YFE0112200], the Guangzhou Science and Technology Project [Grant number 202103000091], the ICTS "NANBIOSIS", in particular by the Drug Formulation Unit (U10) of the CIBER in Bioengineering, Biomaterials and Nanomedicine (CIBER-BBN) at the University of the Basque Country (UPV/EHU), and the Guangzhou Science and Technology Project [Grant number 2023A03J0299].

CRediT authorship contribution statement

Fengjie Liu: Conceptualization, Data curation, Writing – original draft, Visualization. **Yuanyuan Huang:** Methodology. **Xiujuan Lin:** Methodology. **Qianwen Li:** Validation, Writing – original draft, Visualization. **Idoia Gallego:** Writing – review & editing, Visualization. **Guoqiang Hua:** Writing – review & editing, Visualization. **Nadia Benkirane-Jessel:** Writing – review & editing, Visualization. **José Luis Pedraz:** Writing – review & editing, Visualization. **Panpan Wang:** Funding acquisition. **Murugan Ramalingam:** Writing – review & editing. **Yu Cai:** Conceptualization, Data curation, Writing – review & editing, Supervision, Project administration, Funding acquisition.

Declaration of Competing Interest

The authors declare that they have no known competing financial interests or personal relationships that could have appeared to influence the work reported in this paper.

Acknowledgments

Not applicable.

References

Aggarwal, P., Hall, J.B., McLeland, C.B., Dobrovolskaia, M.A., McNeil, S.E., 2009. Nanoparticle interaction with plasma proteins as it relates to particle biodistribution, biocompatibility and therapeutic efficacy. Adv. Drug Deliv. Rev. 61 (6), 428–437.
Barbero, F., Russo, L., Vitali, M., et al., 2017. Formation of the Protein Corona: the Interface between nanoparticles and the immune system. Semin. Immunol. 34, 52–60.
Barré, J., Chamouard, J.M., Houin, G., Tillement, J.P., 1985. Equilibrium dialysis, ultrafiltration, and ultracentrifugation compared for determining the plasma-protein-binding characteristics of valproic acid. Clin. Chem. 31 (1), 60–64.
Chen, D., Ganesh, S., Wang, W., Amiji, M., 2020. Protein corona-enabled systemic delivery and targeting of nanoparticles. AAPS J. 22 (4), 83.
Dewi, C., Fristiohady, A., Amalia, R., Khairul Ikram, N.K., Ibrahim, S., Muchtaridi, M., 2022. Signaling pathways and natural compounds in triple-negative breast cancer cell line. Molecules 27 (12).
Ding, H., Tan, P., Fu, S., et al., 2022. Preparation and application of pH-responsive drug delivery systems. J. Control. Release off. J. Control. Release Soc. 348, 206–238.
Du, M., Ouyang, Y., Meng, F., et al., 2019. Polymer-lipid hybrid nanoparticles: a novel drug delivery system for enhancing the activity of Psoralen against breast cancer. Int. J. Pharm. 561, 274–282.
Filippov, S.K., Khusnutdinov, R., Murmiliuk, A., et al., 2023. Dynamic light scattering and transmission electron microscopy in drug delivery: a roadmap for correct characterization of nanoparticles and interpretation of results. Mater. Horizons 10 (12), 5354–5370.
Giaquinto, A.N., Sung, H., Miller, K.D., et al., 2022. Breast Cancer Statistics, 2022. CA. Cancer J. Clin. 72 (6), 524–541.
Gou, K., Xin, W., Lv, J., et al., 2023. A pH-responsive chiral mesoporous silica nanoparticles for delivery of doxorubicin in tumor-targeted therapy. Colloids Surf. B. Biointerfaces 221, 113027.
Han, H., Li, S., Zhong, Y., et al., 2022. Emerging pro-drug and nano-drug strategies for gemcitabine-based cancer therapy. Asian J. Pharm. Sci. 17 (1), 35–52.
Hoshyar, N., Gray, S., Han, H., Bao, G., 2016. The effect of nanoparticle size on in vivo pharmacokinetics and cellular interaction. Nanomedicine (Lond) 11 (6), 673–692.
Hu, C., Qian, A., Wang, Q., et al., 2016. Industrialization of lipid nanoparticles: from laboratory-scale to large-scale production line. Eur. J. Pharm. Biopharm. Off. J. Arbeitsgemeinschaft Fur Pharm. Verfahrenstechnik E.v 109, 206–213.
Huang, Q., Cai, T., Li, Q., et al., 2018. Preparation of psoralen polymer-lipid hybrid nanoparticles and their reversal of multidrug resistance in MCF-7/ADR cells. Drug Deliv. 25 (1), 1056–1066.
Jin, L., Ma, X.-M., Wang, T.-T., et al., 2020. Psoralen Suppresses Cisplatin-Mediated Resistance and Induces Apoptosis of Gastric Adenocarcinoma by Disruption of the miR196a-HOXB7-HER2 Axis. Cancer Manag. Res. 12, 2803–2827.
Li, Q., Cai, T., Huang, Y., Xia, X., Cole, S.P.C., Cai, Y., 2017. A Review of the structure, preparation, and application of NLCs, PNPs, and PLNs. Nanomater. (Basel, Switzerland) 7.
Li, M., Jia, L., Xie, Y., et al., 2023. Lyophilization process optimization and molecular dynamics simulation of mRNA-LNPs for SARS-CoV-2 vaccine. Npj Vaccines 8 (1), 153.
Li, L., Zou, T., Liang, M., et al., 2021. Screening of metabolites in the treatment of liver cancer xenografts HepG2/ADR by psoralen-loaded lipid nanoparticles. Eur. J. Pharm. Biopharm. Off. J. Arbeitsgemeinschaft Fur Pharm. Verfahrenstechnik E.v 165, 337–344.
Liu, F., Li, L., Lan, M., et al., 2021. Psoralen-loaded polymeric lipid nanoparticles combined with paclitaxel for the treatment of triple-negative breast cancer. Nanomedicine (Lond) 16 (27), 2411–2430.
Liu, H., Zhuang, Y., Wang, P., et al., 2021. Polymeric lipid hybrid nanoparticles as a delivery system enhance the antitumor effect of emodin in vitro and in vivo. J. Pharm. Sci. 110 (8), 2986–2996.
Meng, F., Liu, F., Lan, M., et al., 2021. Preparation and evaluation of folate-modified albumin baicalin-loaded nanoparticles for the targeted treatment of breast cancer. J. Drug Deliv. Sci. Technol. 65, 102603.

Mitrović, J.R., Bjelošević Žiberna, M., Vukadinović, A., et al., 2023. Freeze-dried nanocrystal dispersion of novel deuterated pyrazoloquinolinone ligand (DK-I-56-1): Process parameters and lyoprotectant selection through the stability study. Eur. J. Pharm. Sci. Off. J. Eur. Fed. Pharm. Sci. 189, 106557.
Pan, M.-S., Cao, J., Fan, Y.-Z., 2020. Insight into norcantharidin, a small-molecule synthetic compound with potential multi-target anticancer activities. Chin. Med. 15, 55.
Panno, M.L., Giordano, F., 2014. Effects of psoralens as anti-tumoral agents in breast cancer cells. World J. Clin. Oncol. 5 (3), 348–358.
Pu, Z., Ge, F., Wang, Y., et al., 2021. Ginsenoside-Rg3 inhibits the proliferation and invasion of hepatoma carcinoma cells via regulating long non-coding RNA HOX antisense intergenic. Bioengineered 12 (1), 2398–2409.
Saha, S., Yakati, V., Shankar, G., et al., 2020. Amphetamine decorated cationic lipid nanoparticles cross the blood-brain barrier: therapeutic promise for combating glioblastoma. J. Mater. Chem. B 8 (19), 4318–4330.
Sainaga Jyothi, V.G.S., Bulusu, R., Venkata Krishna Rao, B., et al., 2022. Stability characterization for pharmaceutical liposome product development with focus on regulatory considerations: an update. Int. J. Pharm. 624, 122022.
Sánchez-Iglesias, A., Grzelczak, M., Altantzis, T., et al., 2012. Hydrophobic interactions modulate self-assembly of nanoparticles. ACS Nano 6 (12), 11059–11065.
Shi, P., Cheng, Z., Zhao, K., et al., 2023. Active targeting schemes for nano-drug delivery systems in osteosarcoma therapeutics. J. Nanobiotechnol. 21 (1), 103.
Shi, J., Kantoff, P.W., Wooster, R., Farokhzad, O.C., 2017. Cancer nanomedicine: progress, challenges and opportunities. Nat. Rev. Cancer 17 (1), 20–37.
Shi, L., Xie, Y., Liao, X., Chai, Y., Luo, Y., 2015. Shenmai injection as an adjuvant treatment for chronic cor pulmonale heart failure: a systematic review and meta-analysis of randomized controlled trials. BMC Complement. Altern. Med. 15, 418.
Siegel, R.L., Miller, K.D., Fuchs, H.E., Jemal, A., 2022. Cancer statistics, 2022. CA. Cancer J. Clin. 72 (1), 7–33.
Solomon, D., Gupta, N., Mulla, N.S., Shukla, S., Guerrero, Y.A., Gupta, V., 2017. Role of in vitro release methods in liposomal formulation development: challenges and regulatory perspective. AAPS J. 19 (6), 1669–1681.
Song, Q., Zhang, J., Wu, Q., Li, G., Leung, E.-L.-H., 2020. Kanglaite injection plus fluorouracil-based chemotherapy on the reduction of adverse effects and improvement of clinical effectiveness in patients with advanced malignant tumors of the digestive tract: A meta-analysis of 20 RCTs following the PRISMA guid. Medicine (baltimore). 99 (17), e19480.
Sudhakaran, S., Athira, S.S., Varma, H.K., Mohanan, P.V., 2020. Determination of the bioavailability of zinc oxide nanoparticles using ICP-AES and associated toxicity. Colloids Surf. B. Biointerfaces 188, 110767.
Wang, Y., Sun, T., Jiang, C., 2022. Nanodrug delivery systems for ferroptosis-based cancer therapy., Netherlands.
Wang, X., Xu, C., Hua, Y., et al., 2016. Exosomes play an important role in the process of psoralen reverse multidrug resistance of breast cancer. J. Exp. Clin. Cancer Res. 35 (1), 186.
Wang, X., Xu, C., Hua, Y., et al., 2018. Psoralen induced cell cycle arrest by modulating Wnt/β-catenin pathway in breast cancer cells. Sci. Rep. 8 (1), 14001.
Wang, X., Peng, P., Pan, Z., Fang, Z., Lu, W., Liu, X., 2019. Psoralen inhibits malignant proliferation and induces apoptosis through triggering endoplasmic reticulum stress in human SMMC7721 hepatoma cells. Biol. Res. 52 (1), 34.
Xiao, Z., Wang, C., Li, L., et al., 2018. Clinical efficacy and safety of aidi injection plus docetaxel-based chemotherapy in advanced nonsmall cell lung cancer: a meta-analysis of 36 randomized controlled trials. Evid. Based. Complement. Alternat. Med. 2018, 7918258.
Yang, P., Zhang, L., Wang, T., et al., 2020. Doxorubicin and edelfosine combo-loaded lipid-polymer hybrid nanoparticles for synergistic anticancer effect against drug-resistant osteosarcoma. Onco. Targets. Ther. 13, 8055–8067.
Ye, J., Li, L., Yin, J., et al., 2022. Tumor-targeting intravenous lipid emulsion of paclitaxel: Characteristics, stability, toxicity, and toxicokinetics. J. Pharm. Anal. 12 (6), 901–912.
Yuan, Y., Chiba, P., Cai, T., et al., 2018. Fabrication of psoralen-loaded lipid-polymer hybrid nanoparticles and their reversal effect on drug resistance of cancer cells. Oncol. Rep. 40 (2), 1055–1063.
Yuan, Y., Cai, T., Callaghan, R., et al., 2019. Psoralen-loaded lipid-polymer hybrid nanoparticles enhance doxorubicin efficacy in multidrug-resistant HepG2 cells. Int. J. Nanomedicine 14, 2207–2218.
Zhang, L., Chan, J.M., Gu, F.X., et al., 2008. Self-assembled lipid–polymer hybrid nanoparticles: a robust drug delivery platform. ACS Nano 2 (8), 1696–1702.
Zhang, H., Chen, T., Shan, L., 2019. ShenQi FuZheng injection as an adjunctive treatment to chemotherapy in breast cancer patients: a meta-analysis. Pharm. Biol. 57 (1), 612–624.
Zhao, X., Xu, B., Wu, P., et al., 2020. UHPLC-MS/MS method for pharmacokinetic and bioavailability determination of five bioactive components in raw and various processed products of Polygala tenuifolia in rat plasma. Pharm. Biol. 58 (1), 969–978.
Zou, T., Lu, W., Mezhuev, Y., et al., 2021. A review of nanoparticle drug delivery systems responsive to endogenous breast cancer microenvironment. Eur. J. Pharm. Biopharm. Off. J. Arbeitsgemeinschaft Fur Pharm. Verfahrenstechnik E.v 166, 30–43.